Stacking ensemble of machine learning methods for landslide susceptibility mapping in Zhangjiajie City, Hunan Province, China

Yuke Huan [1], Lei Song [2], Umair Khan [1] and Baoyi Zhang [1,*]

1. *Key Laboratory of Metallogenic Prediction of Nonferrous Metals and Geological Environment Monitoring (Ministry of Education)/ School of Geosciences and Info-Physics, Central South University, Changsha 410083, China.; 205012144@csu.edu.cn (Y.H.); Umair77@csu.edu.cn (U.K.)*

2. *Hunan Institute of Geological Disaster Investigation and Monitoring, Changsha 410004, China; 894469474@qq.com (L.S.);*

* *Correspondence: zhangbaoyi@csu.edu.cn; Tel.: +86-731-88877676 (B.Z.)*

Abstract: The current study aims to apply and compare the performance of six machine learning algorithms, including three basic classifiers: random forest (RF), gradient boosting decision tree (GBDT), and extreme gradient boosting (XGB), as well as their hybrid classifiers, using the logistic regression (LR) method (RF+LR, GBDT+LR, and XGB+LR), in order to map the landslide susceptibility of Zhangjiajie City, Hunan Province, China. First, a landslide inventory map was created with 206 historical landslide points and 412 non-landslide points, which was randomly divided into two datasets for model training (80%) and model testing (20%). Second, a landslide factor database was initially established by selecting 15 landslide conditioning factors from the topography, hydrology, climate, geology, and artificial activities. Thereafter, the multicollinearity test and information gain ratio (IGR) technique were applied to rank the importance of the factors. Subsequently, we used a series of metrics (e.g., accuracy, precision, recall, f-measure, area under the ROC (receiver operating characteristic) curve (AUC), kappa index, mean absolute error (MAE), and root mean square error (RMSE)) to evaluate the accuracy and performance of the six models. Based on the AUC values derived from the models, the GBDT+LR model with the highest AUC value (0.8168) was identified as the most efficient model for mapping landslide susceptibility, followed by the XGB+LR, XGB, RF+LR, GBDT, and RF models, which achieved AUC values of 0.8124, 0.8118, 0.8060, 0.7927, and 0.7883, respectively. The results from this study suggest that the stacking ensemble machine learning method is promising for use in landslide susceptibility mapping in the Zhangjiajie area and is capable of targeting the areas prone to landslides.

Keywords: landslide susceptibility; stacking ensemble; machine learning; random forest; gradient boosting decision tree; extreme gradient boosting

Declarations

Funding: This study was supported by grants from the Hunan Provincial Natural Resource Science and Technology Planning Program of China (Grant No. 2021-53), the National Natural Science Foundation of China (Grant Nos. 42072326 and 41772348), and the National Key Research and Development Program of China (Grant No. 2019YFC1805905).

Conflicts of interest/Competing interests: The authors declare no conflicts of interest and competing interests.

Author Contributions: Conceptualization, Y.H. and B.Z.; methodology, Y.H.; software, Y.H. and U.K.; validation, B.Z.; investigation, L.S.; data curation, L.S.; writing—original draft preparation, Y.H. and U.K.; writing—review and editing, B.Z.; funding acquisition, B.Z. All authors have read and agreed to the published version of the manuscript.

Data Availability Statement: The dataset of the current study is not publicly available due to a data privacy agreement we signed with the Hunan Provincial Planning Institute of Land and Resources, but are available from the corresponding author on reasonable request.

1. Introduction

Landslides describe various processes that lead to the downward and outward movement of slope-forming materials, including rock, soil, and artificial fill, or a combination of these (Cruden and Varnes, 1996). Different natural phenomena and artificial disturbances cause landslides. Natural triggers include meteorological changes (e.g., heavy rainfall or snowmelt) and rapid tectonic forcings (e.g., earthquakes or volcanic eruptions). Artificial disturbances includes land-use change, deforestation, excavation, slope profile change, irrigation, etc. (Guzzetti et al., 2005). Landslides are the seventh most destructive natural disaster globally, destroying transportation, farmland, and villages, and causing loss of life or property, and economic collapse (Petley, 2012).

Landslide susceptibility refers to the probability of landslide occurring in a certain area based on the influence of artificial, terrain, and environmental conditions; that is, the probability of slope damage given certain artificial and natural conditions (Guzzetti et al., 2006). Landslide susceptibility mapping (LSM) in a geographic information system (GIS)-integrated environment is the key to formulating disaster prevention measures and reducing future risks.

Generally, specific methods developed for LSM include: (1) inventory-based and knowledge-driven methods, such as the analytic hierarchy process (Sur et al., 2020); (2) bivariate and multivariate statistical methods, such as frequency ratio (Abedini and Tulabi, 2018), statistical index (Nahayo et al., 2019), evidential belief function

(Mondal and Mandal, 2020), index of entropy (Demir, 2019), weighted linear combination (Gigović et al., 2019), certainty factors (Lin et al., 2021), logistic regression (Kalantar et al., 2018 , Hong et al., 2016), weights-of-evidence (Aghdam et al., 2017), and fuzzy logic (Zhao et al., 2021); (3) machine learning methods, such as support vector machines (Kalantar et al., 2018), artificial neural network (Sadighi et al., 2020 , Kalantar et al., 2018), and decision tree (Pham et al., 2020a). It has been documented that machine learning methods produce more accurate LSM predictions than statistical techniques when evaluating parameters with different statistical distributions and complex feature spaces (Chen et al., 2020b).

Previous comparative studies have found that machine learning models based on ensemble learning are superior to single machine learning models in accuracy and robustness, which can increase the availability of high-resolution LSM (Merghadi et al., 2020 , Sadighi et al., 2020 , Pham et al., 2017). In particular, some ensemble learning algorithms based on decision tree (DT) have improved the accuracy and efficiency of landslide classification (Merghadi et al., 2020). DT is a basic classifier of various bagging (Breiman, 1996) and boosting (Freund, 1990) ensemble machine learning algorithms. Kadavi et al. (2019) applied a DT classification method to predict the areas with high potential for future landslide occurrence and reported that the prediction accuracy of the DT model is better than the LR model. Bagging, which stands for boostrap aggregation, is a technique for repeated sampling with put-back from data based on a uniform probability distribution (Breiman, 1996). Random forest (RF) is a typical bagging ensemble machine learning model consisting of DTs that can be trained independently or in parallel (Breiman, 2001). Thai Pham et al. (2018) applied different machine learning algorithms for the modeling of landslide susceptibility in the Luc Yen district, Northern Vietnam, and found that the RF method could be applied for better landslide susceptibility mapping and management. Lai and Tsai (2019) developed a systematic approach with the RF method to apply satellite remote sensing images, geographic information system (GIS) datasets, and spatial analysis for multi-temporal and event-based landslide susceptibility assessments on a regional scale. Unlike bagging, boosting is a weight-based integration of multiple resampled weak classifiers to form a strong classifier (Freund, 1990). Boosting ensemble machine learning models, such as AdaBoost (Pham et al., 2015), MultiboostAB (Webb, 2000), the gradient boosting decision tree (GBDT) (Jerome, 2001), and extreme gradient boosting (XGB) (Chen and Guestrin, 2016), are widely used in landslide susceptibility prediction. Chen et al. (2020a) reported that the GBDT method outperformed the other machine learning methods, and was able to provide strong technical support for producing landslide susceptibility maps in the Three Gorges Reservoir (TGR) area. Sahin (2020) produced a landslide susceptibility map using three featured

regression DT-based ensemble methods, including GBDT, XGB, and RF, and the results showed that the XGB method achieved a lower prediction error and higher accuracy than the other ensemble methods.

The aforementioned bagging and boosting ensemble learning methods are homogeneous in that they combine several identical models into one prediction method. However, due to the heterogeneity of topographic, geological, hydrological, and artificial conditions in different landslide areas, homogeneous ensemble learning may not be suitable for all LSM scenarios. Stacking is a typical heterogeneous classifier composition framework proposed by Wolpert (1992). By generalizing the outputs of multiple classifiers, a stacking ensemble uses the outputs of the previous classifier as the learning input information of the next layer so that the previous learning can be fully used in the subsequent induction process to discover and correct classification deviations, in order to achieve higher classification accuracy than the single classifiers. Althuwaynee et al. (2014) proved the efficiency and reliability of ensemble DT and LR models in LSM. He et al. (2014) introduced a model that combines GBDT with LR, outperforming either of these methods on its own by over 3%. Ma et al. (2015) proposed a novel framework to identify gene variation using LR and RF. According to the above literature results, it is feasible to stack DT-based machine learning models with a logistic regression model to improve the prediction accuracy and performance of landslide susceptibility prediction models.

The current study aims to carry out LSM for Zhangjiajie City, Hunan Province, China, and to improve LSM effectiveness for decision-makers. In order to achieve this purpose, the RF, GBDT, and XGB methods were used for LSM and compared with the hybrid models RF+LR, GBDT+LR, and XGB+LR. Whereafter, we used a series of criteria to evaluate the performance of the six models, including accuracy, precision, recall, f-measure, area under the ROC (receiver operating characteristic) curve (AUC), kappa index, and root mean square error (RMSE). In addition, the frequency ratio method was used to conduct quantitative analysis on the prediction effect of each machine learning model. Finally, based on the above evaluations, suggestions were drawn for landslide disaster risk prevention and management in the study area.

2. Study Area and Dataset

2.1. Study Area

There are a total of 18,567 potential geological disaster sites in Hunan Province, accounting for 6.5% of the total sites and ranking fourth in China, threatening a population of 712,600 people and property worth CNY 29.824 billion. The types of potential disaster sites in Hunan Province are mainly landslides, with a total of 11,405 sites. Therefore, Zhangjiajie City is one of the key objects of geological disaster prevention and control in Hunan Province.

Zhangjiajie City (located between 28°52′ and 29°48′ north latitude, 109°40′ and 111°20′ east longitude) is in the northwest part of Hunan Province with an area of 9516 km2 (Fig. 1). The elevation ranges from 67 to 1840 m above sea level (asl). Notable alluvial terraces and karst landscapes have been formed in the Zhangjiajie area, located in the Wuling Range between the Yun-Gui Plateau to the northeast and the mountainous area of northwestern Hunan Province, with the mountainous area accounting for 76% of the total area (Yang et al., 2011). The lithostratigraphy within this area is comprised of Silurian, Devonian, Permian, Triassic, and Quaternary strata. The Silurian and Devonian strata account for most of the total area (Hunan Bureau of Geology and Mineral Resources, 1988). The study area belongs to the mid-tropical monsoon climate, with abundant and concentrated precipitation, with an average annual precipitation of 1200–1500 mm. Rainfall is an important external condition for the occurrence and development of landslides in the study area, especially the shallow accumulation body. The rivers and streams in Zhangjiajie City are crisscrossed, and the water system is dominated by the Lishui River and the Loushui River. The largest land-use types in Zhangjiajie City are forest land and cropland. The permanent resident population of Zhangjiajie City has reached more than 1.51 million.
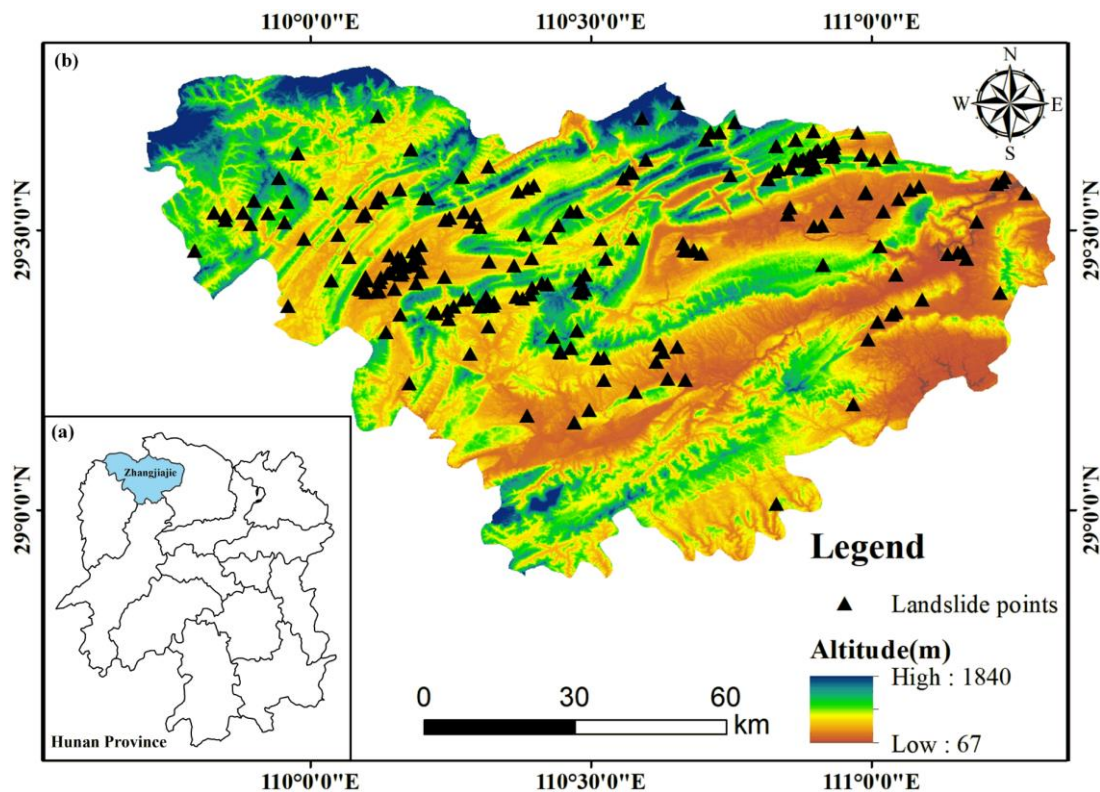
Fig 1. Location map of the study area: (a) location of the study area in Hunan Province, and (b) elevation of the study area along with location of landslide points in that.

2.2. Dataset

In this study, a landslide inventory map containing 206 historical landslide sites in the Zhangjiajie City of Hunan Province, China was get based on field survey and high-resolution remote sensing image interpretation carried out by the Hunan Institute of Geological Survey (oa.hnsddy.com, Changsha, China). Most of these historical landslides belong to small and medium-sized scale, and the general movement type is clay/silt sliding with the characteristics of high frequency and wide distribution, which can be classified as shallow soil landslide according to the classification standard of landslides (Hungr et al., 2014). Landslide points and non-landslide points are extracted as positive and negative samples, respectively. To avoid the close proximity of the positive and negative samples, 412 non-landslide points were randomly extracted outside the 1000 m buffer zone of the landslide sites. Subsequently, 80% of the points were chosen for model training and 20% for testing.

Based on the existing literature and data availability, we chose 15 conditioning factors from multi-disciplines that have an effect on the occurrence of landslide, such as geomorphology, hydrology, climate, geology, and artificial activities. These LCFs include altitude, slope, aspect, plane curvature, profile curvature, relief, roughness, rainfall, topographic wetness index (TWI), normalized difference vegetative index (NDVI), distance to roads, distance to rivers, land use/land cover (LULC), soil texture, and lithology (Tables 1 and 2). All the LCFs were converted into a raster form with a spatial resolution of 90 m (Fig. 2).

Table 1 The landslide conditioning factors (LCFs) used in this study.

NO.	LCF	Classes	Data source	Resolution (Scale)	Description
1	Altitude (m)	67–317, 317–527, 527–750, 750–1037, and 1037–1840.	Digital elevation model (DEM)	90 × 90 m	Affecting rainfall and related surface runoff (Botzen et al., 2013).
2	Slope (°)	0–8.382, 8.382–15.680, 15.680–23.664, 23.664–33.440, and 33.440–71.275.	DEM	90 × 90 m	Influencing slope stability as well as surface runoff, infiltration, and drainage density (Nefeslioglu et al., 2008).
3	Aspect	flat (–1), north (0–22.5°), northeast (22.5–67.5°), east (67.5–112.5°), southeast (112.5–157.5°), south	DEM	90 × 90 m	The orientation of the slope.

		(157.5–202.5°), southwest (202.5–247.5°), west (247.5–292.5°), northwest (292.5–337.5°), and north (337.5–360°).			
4	Plane curvature	−6.555 to −0.460, −0.460 to 0.120, −0.120 to 0.137, 0.137 to 0.478, and 0.478 to 4.314.	DEM	90 × 90 m	Reflecting the divergence and convergence of water on the surface (Huang et al., 2020).
5	Profile curvature	−5.902 to −0.569, −0.569 to 0.178, −0.178 to 0.116, 0.116 to 0.507, and 0.507 to 6.575.	DEM	90 × 90 m	Affecting the flow velocity variation of slope (Pham et al., 2017).
6	Relief (m)	0-45, 45-80, 80-120, 120-176, and 176-756.	DEM	90 × 90 m	Difference of the maximum and minimum elevations within a certain area.
7	Roughness	1–1.054, 1.054–1.137, 1.137–1.261, 1.261–1.509, and 1.509–3.321.	DEM	90 × 90 m	Undulation changes and erosion degree of the ground surface.
8	Rainfall (mm/yr)	0–1000, 1000–1200, 1200–1400, 1400–1600, and 1600–2000.	Hunan Provincial Institute of Land Resources Planning (www.hngtghy.com, Changsha, China)	1000 × 1000 m	An important external condition.
9	TWI	−1.025–3.277, 3.277–6.456, 6456–9.542, 9.542–12.067, and 12.067–22.822.	DEM	90 × 90 m	Predicting areas susceptible to the surface of saturated soil.
10	NDVI	0.244–0.500, 0.500–0.632, 0.632–0.736, 0.736–0.816, and 0.816–0.900.	Resource and Environment Science Data Center (www.resdc.cn, Beijing, China)	30 × 30 m	Measuring the degree of vegetation coverage and the status of vegetation growth (Tien Bui et al., 2019).

11	Distance to rivers (m)	0–603.738, 603.738–1297.998, 1297.998–2012.461, 2012.461–2747.58, 2747.581–3520.369, 3520.369–4374.037, 4374.037–5331.313, 5331.313–6468.114, and 6468.114–9198.070.	OpenStreetMap (www.openhistoricalmap.org, Cambridge, UK)	90 × 90 m	Erosion of river.
12	Distance to roads (m)	0–576.281, 576.281–1297.998, 1297.998–2056.259, 2056.259–2871.550, 2871.550–3798.171, 3798.171–4923.749, 4923.749–6321.179, 6321.179–8375.321, and 8315.321–11783.128.	OpenStreetMap	90 × 90 m	Reflecting the intensity of human influence.
13	LULC	cropland, forests, grassland, wetland, water bodies, and artificial surfaces.	GLOBELAND30 (www.globallandcover.com, Beijing, China)	30 × 30 m	The soil properties of cohesive force, friction angle, soil bulk density, and pore pressure will change under different land covers (Nguyen et al., 2019).
14	Soil texture	haplic acrisols, humic acrisols, ferric alisols, haplic alisols, cumulic anthrosols, dystric cambisols, ferralic cambisols, rendzic leptosols, haplic luvisols, chromic luvisols, ferric lixisols, calcaric regosols, dystric regosols, and water bodies.	Harmonized World Soil Database (HWSD) built by the Food and Agriculture Organization of the United Nations (UNFAO, www.fao.org, Rome, Italy) and the International Institute for Applied Systems Analysis (IIASA, iiasa.ac.at, Laxenburg, Austria)	1:5000000	Representing the texture of the soil materials that influence landslide occurrence.

| 15 | Lithology | As shown in Table 2. | Geological map database of China | 1:500000 | Influencing the occurrence of erosion, ground stability, and landslide (Arulbalaji et al., 2019). |

Table 2 Lithological units and their description of the study area.

	Lithological Unit	Description	Age Era
1	K_2	Red sandstone, calcium mudstone, glutenite.	Cretaceous
2	K_1	Red siltstone, mudstone, glutenite, basalt.	Cretaceous
3	K	Union layer.	Cretaceous
4	J_{1+2}	Upper and middle series coexisted.	Jurassic
5	J_1	Sandstone, feldspar quartz sandstone, shale, conglomerate, basalt.	Jurassic
6	T_3	Sandstone, mudstone, shale, quartz conglomerate.	Triassic
7	T_2	Variegated calcareous mudstone, siltstone, dolomite.	Triassic
8	T_1	Limestone, dolomite, argillaceous limestone.	Triassic
9	P	Upper series: siliceous rock, shale, limestone, sandstone; lower series: chert limestone, magnesian marl.	Permian
10	D_{2+3}	Middle series and lower series cobedded.	Devonian
11	D_1	Purple sandstone, shale, glutenite.	Devonian
12	S	Siltstone, shale, sandy limestone, shell limestone.	Silurian
13	O	Parallel beds.	Ordovician
14	ϵ_3	Dolomite, limestone.	Cambrian
15	ϵ_{2+3}	Syncretism of the upper and middle series.	Cambrian
16	ϵ_2	Limestone, dolomite, shale.	Cambrian
17	ϵ_1	Limestone, marl, shale, carbonaceous shale.	Cambrian
18	Z	Syncline.	Sinian
19	Pt_3^1bx	Banxi group. Purple slate, metamorphic sandstone, limestone, pebbled sandstone, mafic rock.	Lower Upper Proterozoic
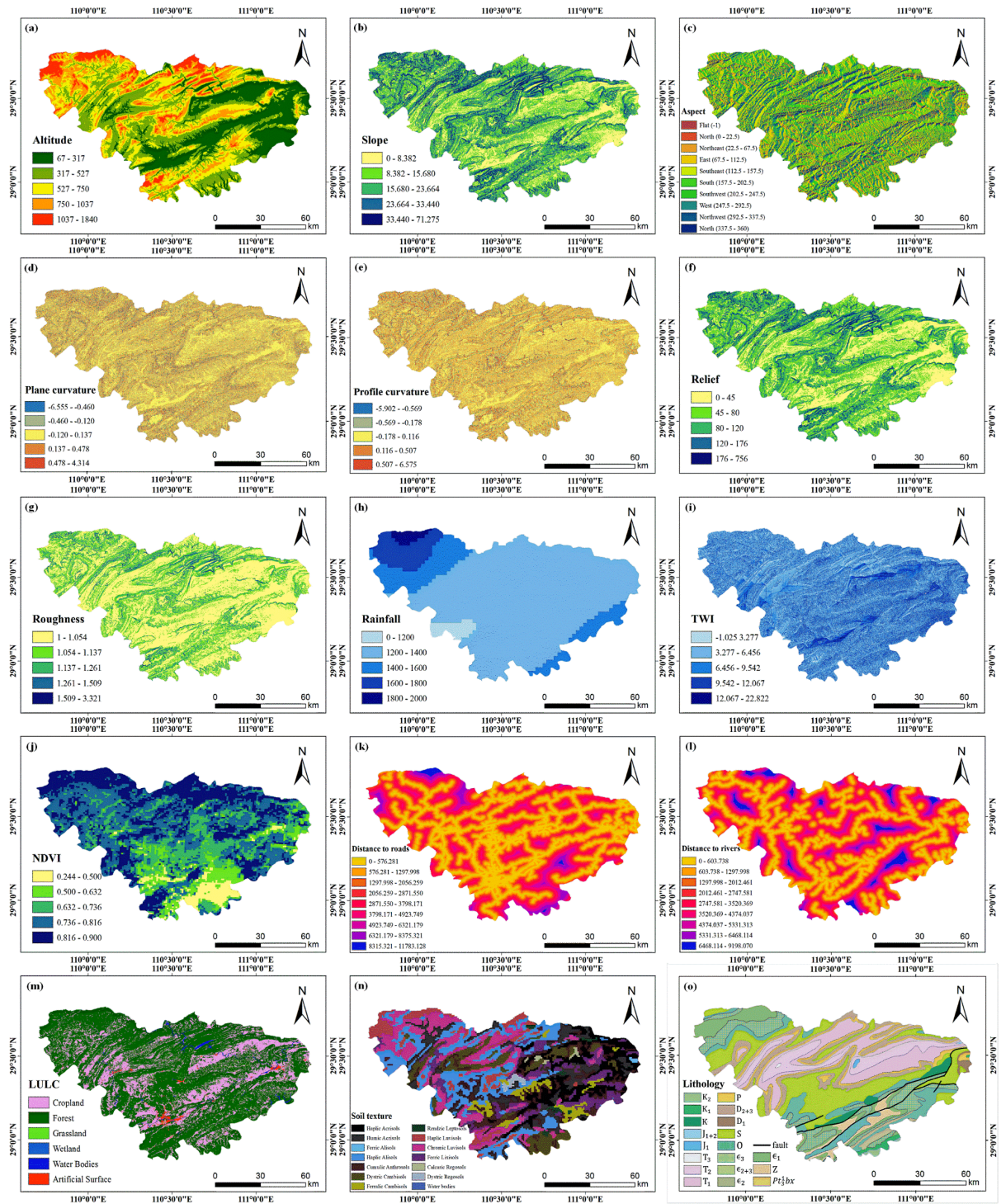
Fig 2. LCFs for landslide susceptibility mapping (LSM): (a) altitude, (b) slope, (c) aspect, (d) plane curvature, (e) profile curvature, (f) relief, (g) roughness, (h) rainfall, (i) topographic wetness index (TWI), (j) normalized difference vegetative index (NDVI), (k) distance to roads, (l) distance to rivers, (m) land use/land cover (LULC), (n) soil texture, and (o) lithology.

3. Methods

The LSM scheme is presented in Fig. 3, and the main procedures are described as follows.

(1) Selecting and ranking LCFs: in total, 15 landslide conditioning factors were selected from topography, hydrology, climate, geology, and artificial activities, which included altitude, slope, aspect, plane curvature, profile curvature, relief, roughness, rainfall, TWI, NDVI, distance to roads, distance to rivers, LULC, soil texture, and lithology. We used multicollinearity analysis to detect factor multicollinearity and information gain ratio (IGR) technology to measure the importance of LCFs, so as to independently evaluate the correlation of factors and eliminate irrelevant or redundant factors.

(2) Modeling: we first used several machine learning methods as basic classifiers to model landslide susceptibility, including the RF model with the bagging method, and the GBDT and XGB models with the boosting method. Subsequently, these DT-based ensemble models were stacked with the logistic regression (LR) linear classifier model, then the RF+LR, GBDT+LR, and XGB+LR models were constructed for landslide susceptibility prediction.

(3) Model validation and comparison: we used a series of machine learning evaluation methods and error-based evaluation methods to measure and compare the performance of the six models, including accuracy, precision, recall, f-measure, area under the ROC (receiver operating characteristic) curve (AUC), kappa index, and root mean square error (RMSE).

(4) Visualization of landslide susceptibility map: we made landslide susceptibility prediction maps to qualitatively evaluate the prediction capabilities of each model, and used the frequency ratio method to quantitatively evaluate the prediction results and overall performance of all models in detail.
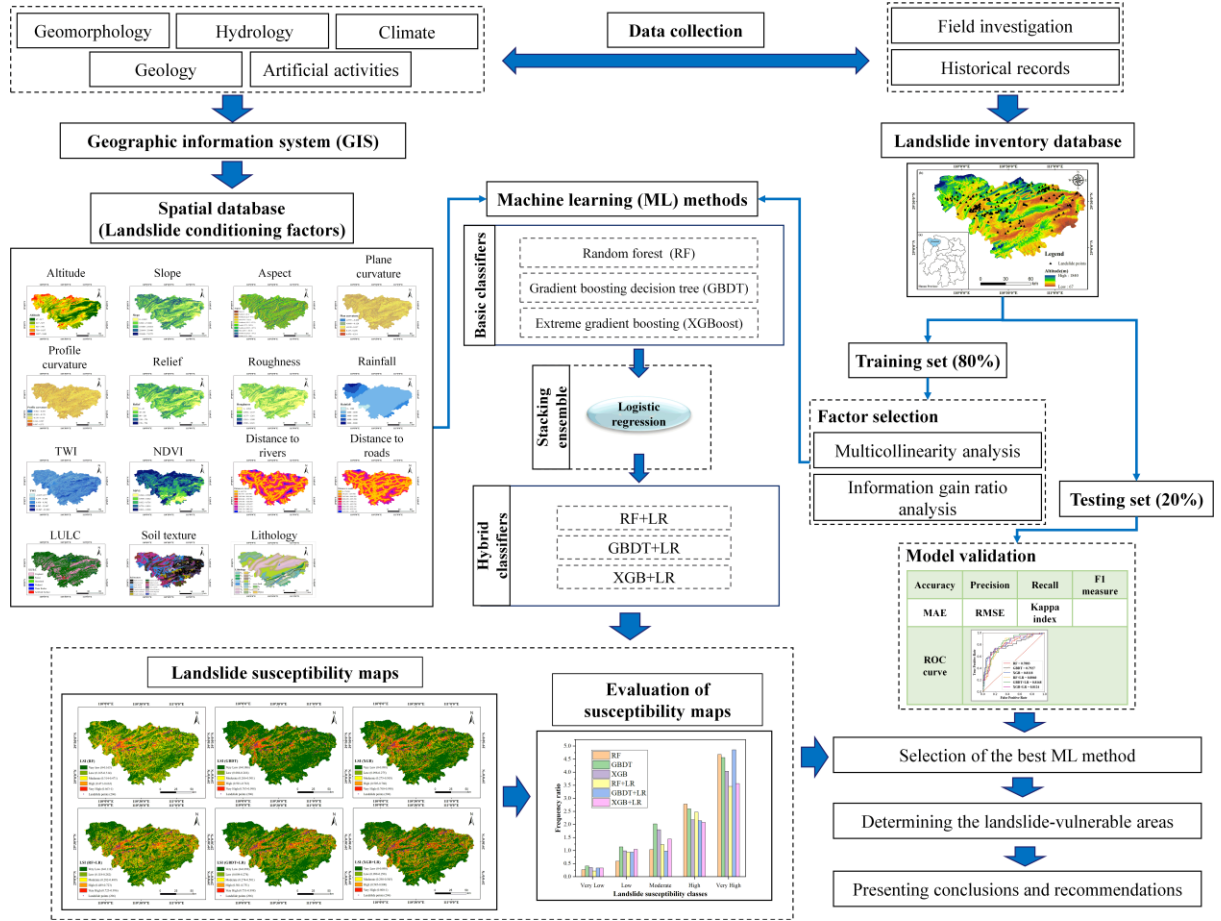
Fig 3. Flowchart of LSM using the stacking ensemble machine learning models.

3.1. Importance Analysis of LCFs

Choosing appropriate landslide conditioning factors (LCFs) as model input is of great significance for landslide susceptibility evaluation. Information gain ratio (IGR) (Nhu et al., 2020a) is the ratio of node information gain to node split information measure. It is a factor ranking technique that can independently evaluate different factors' correlations and detect the irrelevant or redundant factors.

We used the IGR method to rank and choose the factors that affect landslide susceptibility.

It is assumed that T is the total number of input tuples for each factor in the training dataset, T_j is the total number of positive or negative tuples in the training dataset, v is the total number of classes in the dataset, and S is one of the factors influencing landslide disaster. The specific calculation of IGR(S) is as follows:

$$IGR(S) = \frac{Gain(S)}{SplitInfo(S)} \tag{1}$$

where:

$$SplitInfo(S) = -\sum_{j=1}^{v} \frac{|T_j|}{|T|} log_2 \left(\frac{|T_j|}{|T|} \right) \tag{2}$$

$$Gain(S) = I(P, N) - E(S) \tag{3}$$

$$E(S) = -\sum_{i=1}^{k} \frac{P_i + N_i}{P + N} I(P_i, N) \tag{4}$$

$$I(P_i, N) = -\frac{P}{P + N} log_2 \frac{P}{P + N} - \frac{N}{P + N} log_2 \frac{N}{P + N} \tag{5}$$

where: $E(S)$ represents the entropy of the S factor in the training dataset, $I(P,N)$ shows the information required to satisfy the given training dataset, P is the total number of positive tuples in the training dataset, N illustrates the total number of negative tuples in the training dataset, P_i and N_i mean the number of positive and negative tuples of the i-th S factor, respectively, and k represents the number of values of the S factor.

3.2. Multicollinearity Analysis

Multicollinearity refers to the mutual dependence, lack of independence, and complete or nearly complete linear relationship between the variables in the regression equation (Farrar and Glauber, 1967). By analyzing whether there is multicollinearity in the model, high multicollinearity factors should be removed to minimize the bias of the model and to optimize the prediction results. Multicollinearity is usually analyzed by variance inflation factor (VIF) and tolerance (TOL) (Green and Stephenson, 1986). Their equations are as follows:

$$TOL = 1 - R_j^2 \tag{6}$$

$$VIF = \frac{1}{TOL} \tag{7}$$

where: R_j is the negative correlation coefficient between the j-th independent variable x_j and the other independent variables.

The value of VIF increases with the increase of R_j^2. Generally, if the TOL value is <0.10 or 0.20 and the VIF value is >5 or 10, the results indicate a high degree of multicollinearity between variables (Band et al., 2020).

3.3. Basic Classifiers

The RF classifier is an improved form of bagged DT-based classifier, which is used to solve complex problems of prediction and multi-classification. It combines the bagging integrated learning algorithm with the random subspace algorithm, making it a powerful classification tool capable of recognizing large-scale and multivariable data. RF consists of four parts, i.e., random selection of samples (put-back sampling), random selection of features, construction of decision trees, and random forest voting (averaging) (Breiman, 2001).

Gradient boosting decision tree (GDBT) is a multiple decision tree ensemble machine learning method based on a boosting scheme. The GBDT algorithm builds the model by iteratively forming regression DT as a weak classifier. The weak classifier of each round is generated through multiple iterations, trained on the residuals of

the previous round (Jerome, 2001). The GBDT algorithm uses multiple classifiers to create hundreds of trees that can minimize the over-fitting of the decision tree algorithm. Moreover, the design of each sub-classifier is simple, and the training progress can be accelerated accordingly.

Extreme gradient boosting (XGB) is a highly scalable decision tree integrated machine learning method based on the principle of gradient boosting machines (Chen and Guestrin, 2016). The XGB algorithm improves the GBDT by optimizing the function space gradient descent algorithm from a first-order Taylor expansion to a second-order Taylor expansion, and by adding a regular term to avoid over-fitting (Zhang et al., 2021).

The LR method is a predictive analysis process that combines linear regression with a sigmoid function, using events as dependent variables while causal factors in categorical, continuous, or binary variables as independent variables (Hong et al., 2016). In the process of landslide sensitivity analysis, the independent variables are the LCFs, and the dependent variable is the variable of landslide occurrences. The output value of the model is between 0 and 1. Usually, 0 represents a non-landslide event (negative cell), and 1 represents a landslide event (positive cell). The closer the value is to 1, the higher the probability of landslide occurring; on the contrary, the closer the value is to 0, the lower the probability of landslide occurring.

3.4. Stacking Ensemble

The stacking ensemble method is an integration model proposed by Wolpert (1992) for compiling several different algorithms on training processes, which works by estimating raw classifiers with poor performance relative to independent or bootstrapped training data (Dou et al., 2020).

The stacking model fusion system is designed as a two-layer structure, as shown in Fig. 4. The first layer is integrated by N boosted tree models to form the basic classifier layer of the fusion system. The output of each tree is used as the classification input of the second-layer sparse linear classifier, thereby fusing the N basic models. Assuming that the input feature is x_i, the h-th basic classifier in the first layer is F_h, and the meta-classifier in the second layer is F, then the output of the h-th basic classifier of the first layer is $F_h(x_i)$, which is used as the input feature of the meta-classifier of the second layer, and the output y_i is the final prediction result. As shown in Equation (8):

$$y_i = F\big(F_1(x_i), \dots, F_h(x_i)\big), \dots, F_m(x_i) \tag{8}$$

Essentially, the GBDT+LR model is a binary classifier model with a stacking design, so it can be used to solve binary classification problems. The RF+LR and XGB+LR models have therefore been proposed on this basis. The ensemble decision tree is used instead of the single decision tree to build the model because the expression ability of a single tree is not sufficient to express multiple distinguishing feature combinations. The

expression ability of multiple trees can better find effective features and feature combinations.

The detailed process of stacking of the three DT-based basic models with the LR model is shown in Fig. 4. First, after RF random sampling with put-back and GBDT and XGB random sampling without put-back, their respective original training datasets are obtained. Second, the basic model trains the original training dataset and obtains a binary classifier. One-hot encoding is the process of representing categorical variables as binary vectors. When the basic model makes a prediction, the output is not the probability value, but the one-hot coding used to record the position of the leaf node where the predicted probability value of each tree in the model is binarized as 1 or 0. Since each weak classifier has only one leaf node to output the prediction results, while in a basic model, there are a weak classifiers and a total of b leaf nodes, each training data will be converted into a sparse vector of $1 * b$ dimension, in which a elements are 1 and the rest of $b - a$ elements are 0. Thus, a new training dataset is constructed as an input of the LR model. Next, the new training dataset and labels derived from the original training dataset are inputted into the LR classifier for final training. Finally, the prediction results of RF+LR, GBDT+LR, and XGB+LR are obtained. After the basic model extracted the original dataset into a new dataset, not only did the input data of the LR model become sparse, but also, due to the influence of the numbers of weak classifiers and leaf nodes, the feature dimension of the new training data may be too large. Therefore, the regularization method needs to be used in the LR model to reduce the risk of overfitting.
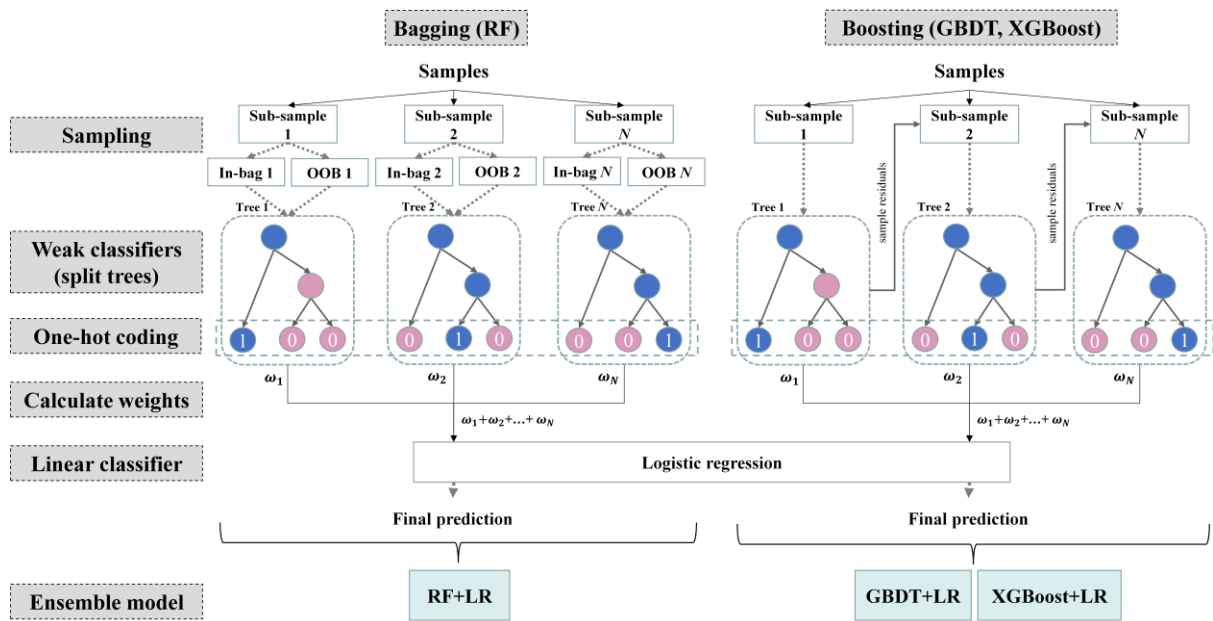
Fig. 4 Stacking ensemble structures for random forest (RF), gradient boosting decision tree (GBDT), and Extreme gradient boosting (XGB) with logistic regression (LR).

4. Results

4.1. Correlation among LCFs

In this study, we used variance inflation factor (VIF) and tolerances (TOL) to evaluate the multicollinearity of LCFs. Table 3 shows the VIF and TOL of the 15 LCFs. The results show that the VIF value of the "relief" factor is greater than 5.0 and has multicollinearity, which needs to be excluded from the LCFs. However, the remaining 14 LCFs have no obvious correlation and can be used as input variables to model landslide susceptibility.

Table 3 Multicollinearity of the LCFs.

Factors	TOL	VIF
Altitude	0.565	1.771
Slope	0.337	2.970
Aspect	0.976	1.024
Profile curvature	0.763	1.311
Plane curvature	0.739	1.353
TWI	0.742	1.347
NDVI	0.834	1.200
Relief	0.194	5.152
Roughness	0.225	4.435
Distance to roads	0.765	1.307
Distance to rivers	0.733	1.364
Rainfall	0.767	1.303
LULC	0.936	1.068
Soil texture	0.905	1.105
Lithology	0.884	1.131

4.2. Importance of LCFs

Table 4 shows the average merit (AM) value of the LCFs calculated using the information gain ratio (IGR) method. The results show that the AM values of all factors are greater than 0; therefore, all factors can be added to the landslide susceptibility modeling process. Among the 15 factors, profile curvature (AM = 0.610) is the most significant factor, followed by roughness (AM = 0.609), LULC (AM = 0.525), altitude (AM = 0.525), distance to roads (AM = 0.443), TWI (AM = 0.358), lithology (AM = 0.339), NDVI (AM = 0.292), slope (AM = 0.291), distance to rivers (AM = 0.200), plane curvature (AM = 0.185), aspect (AM = 0.177), soil texture (AM = 0.176), and rainfall (AM = 0.147).

Table 4 The most effective factors for landslide occurrence.

Factors	Rank	Average merit
Profile curvature	1	0.610

Roughness	2	0.609
LULC	3	0.525
Relief	4	0.443
Altitude	5	0.413
Distance to roads	6	0.364
TWI	7	0.358
Lithology	8	0.339
NDVI	9	0.292
Slope	10	0.291
Distance to rivers	11	0.200
Plane curvature	12	0.185
Aspect	13	0.177
Soil texture	14	0.176
Rainfall	15	0.147

4.3. Validation and Evaluation of Models

In this study, we used RF, GDBT, XGB, RF+LR, GBDT+LR, and XGB+LR models to execute the modeling process on the training set and obtained evaluation results. We applied the 10-fold cross-validation method to prevent overfitting and to reduce model variability, then applied the grid search method to find the best hyper-parameters for each model (Table 5). Accuracy, precision, recall, f-measure, area under the ROC (receiver operating characteristic) curve (AUC), kappa index, mean absolute error (MAE), and root mean square error (RMSE) were used to evaluate the performance of the six models. Higher values of model accuracy, precision, recall, f-measure, AUC, and kappa, as well as lower values of RMSE and MAE, mean better performance of the model.

Table 6 lists the machine learning–based assessment results of five indicators: accuracy, precision, recall, f-measure, and AUC. Both the accuracy and precision values of GBDT+LR are greater than 0.800, which is higher than the other five models. The XGB model yielded the highest recall and f-measure values. In addition, the performance of the RF+LR and GBDT+LR models is better than that of the RF and GBDT models in terms of all the statistical measures. As shown in Fig. 5, the AUC values of the GBDT+LR, XGB+LR, XGB, and RF+LR models are above 0.800, indicating that the above four models demonstrate very satisfactory prediction capability. Furthermore, the GBDT+LR model is better than the other models, due to it obtaining the highest AUC value.

In terms of error-based assessment results (Table 7), the highest kappa index value was obtained by the GBDT+LR model, followed by XGB, GBDT, RF+LR, RF, and XGB+LR models. The kappa index values show

the compatibility and reliability of the LSM models. The MAE and RMSE metrics indicate that the GBDT+LR model has the smallest errors, followed by the XGB, RF+LR, GBDT, RF, and XGB+LR models.

The validation results show that the six models have good performance in landslide prediction. Therein, the GBDT+LR model has the best accuracy and predictive ability compared with the other models. The analysis of the model results also confirms that the stacking ensemble method is a useful tool for improving the accuracy of model prediction.

Table 5 Hyper-parameters of basic classifiers.

Models	Parameters
RF	max_depth = 9, max_features = 0.4, max_leaf_nodes = 100, n_estimators = 20
GBDT	max_depth = 6, max_features = 0.2, max_leaf_nodes = 200, n_estimators = 110
XGB	max_depth = 7, n_estimators = 125, reg_alpha = 0.1, reg_lambda = 0.01, eval_metric = ['logloss','auc','error'], learning_rate = 0.1, n_jobs = –1

Table 6 Evaluation of LSM models using machine learning metrics.

Models	Accuracy	Precision	Recall	F-measure	AUC
RF	0.766	0.710	0.524	0.603	0.788
GBDT	0.774	0.675	0.643	0.659	0.793
XGB	0.790	0.700	0.667	0.683	0.812
RF+LR	0.782	0.742	0.548	0.630	0.806
GBDT+LR	0.806	0.800	0.571	0.667	0.817
XGB+LR	0.758	0.676	0.548	0.605	0.812

Table 7 Evaluation of LSM models using error metrics.

Models	MAE	RMSE	Kappa index
RF	0.234	0.484	0.442
GBDT	0.226	0.475	0.490
XGB	0.210	0.458	0.526
RF+LR	0.218	0.467	0.474
GBDT+LR	0.194	0.440	0.536
XGB+LR	0.242	0.492	0.434
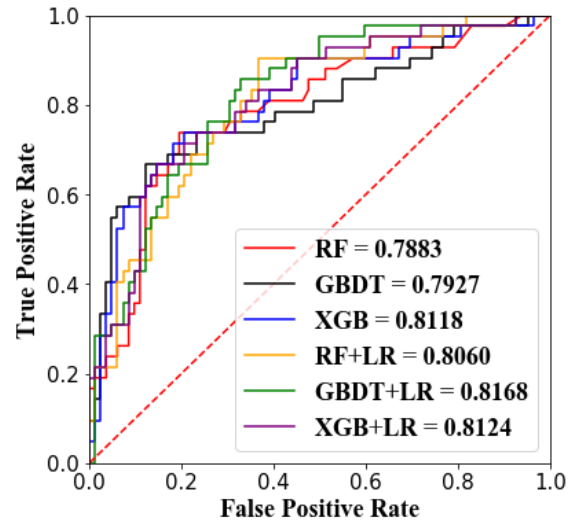
Fig 5. Receiver operating characteristic (ROC) curves of the LSM models.

4.4. Landslide Susceptibility Mapping (LSM)

After training and validating all models, we ran the models and obtained the output weight (i.e., the landslide sensitivity index (LSI)). We mapped the landslide sensitivity of the study area by predicting a LSI value on each pixel in the study area. Ultimately, the natural break classification method was used to classify the landslide susceptibility of the study area into five categories (i.e., very low, low, moderate, high, or very high) (Fig. 6).
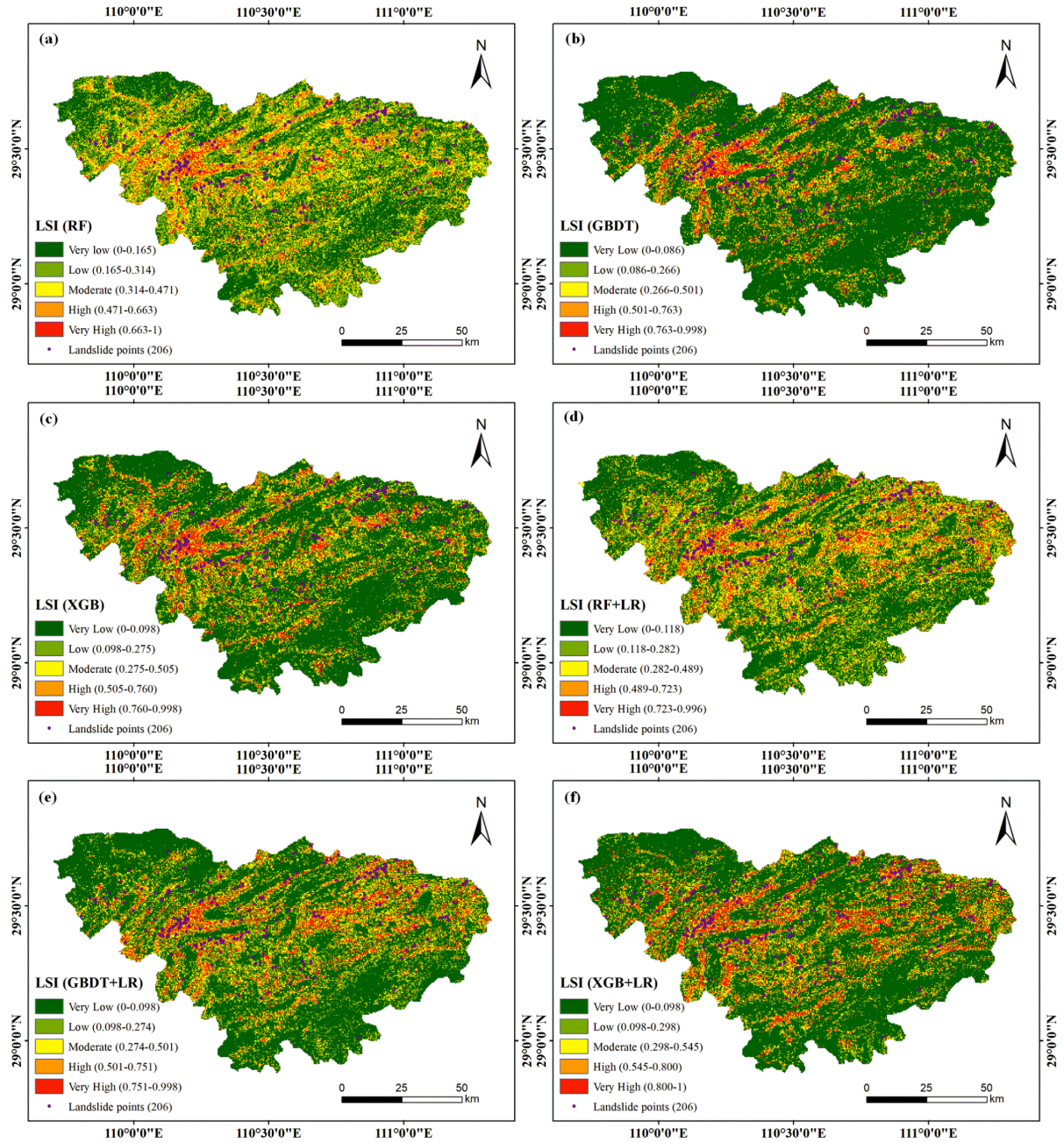
Fig 6. Landslide susceptibility maps using: (a) RF, (b) GBDT, (c) XGB, (d) RF+LR, (e) GBDT+LR, and (f) XGB+LR models.

LSM can only qualitatively assess landslide susceptibility, and further statistical methods can be used for a quantitative assessment (Zhou et al., 2021b). The FR method was used to investigate the separation between classes (i.e., to assess the classification accuracy of the models), which represents the ratio of the percentage of landslides to the percentage of the total area in each class (Arabameri et al., 2019). Generally, models with the characteristics of landslide points concentrated in high-prone areas are considered to have strong landslide prediction ability. As shown in Table 8 and Fig. 7, the low and very low susceptibility categories of the six landslide susceptibility maps account for the majority, exceeding 70%, however, there are fewer landslide points

in these two areas. Conversely, the high and very high susceptibility categories occupy less than 18% of the study area, but all have more than 50% of landslides occurring there. The statistical results show that the FR value gradually increases as the landslide susceptibility level increases from very low to very high, which means the six landslide susceptibility maps are reasonable and reliable.

According to the FR analysis results, the GBDT+LR model has the highest reliability of landslide susceptibility maps compared with the other five models. In the GBDT+LR maps, the percentage of landslide occurrences and the frequency of high susceptibility and very high susceptibility classes are higher than those of other models.

Table 8 Statistics of landslide susceptibility classes with frequency ration (FR).

Models	Class	Area		Landslides		FR
		(km²)	%	Nos	%	
RF	Very Low	3448.01	36.23	20	9.71	0.27
	Low	2911.40	30.59	37	17.96	0.59
	Moderate	1604.37	16.86	36	17.48	1.04
	High	2911.40	11.33	65	31.55	2.78
	Very High	474.33	4.98	48	23.30	4.68
GBDT	Very Low	6547.39	68.80	58	28.16	0.41
	Low	1177.69	12.38	29	14.08	1.14
	Moderate	639.67	6.72	28	13.59	2.02
	High	1177.69	5.60	30	14.56	2.60
	Very High	618.16	6.50	61	29.61	4.56
XGB	Very Low	5711.21	60.02	43	20.87	0.35
	Low	1533.35	16.11	33	16.02	0.99
	Moderate	873.77	9.18	34	16.50	1.80
	High	1533.35	6.89	31	15.05	2.18
	Very High	742.21	7.80	65	31.55	4.04
RF + LR	Very Low	4286.66	45.05	20	9.71	0.22
	Low	2205.66	23.18	45	21.84	0.94
	Moderate	1349.37	14.18	36	17.48	1.23
	High	2205.66	10.03	51	24.76	2.47
	Very High	720.07	7.57	54	26.21	3.46
GBDT + LR	Very Low	5324.97	55.96	38	18.45	0.33
	Low	1719.70	18.07	35	16.99	0.94
	Moderate	984.55	10.35	21	10.19	0.98
	High	1719.70	7.93	35	16.99	2.14
	Very High	732.19	7.69	77	37.38	4.86
XGB + LR	Very Low	5607.03	58.92	40	19.42	0.33

Low	1362.08	14.31	31	15.05	1.05
Moderate	832.00	8.74	26	12.62	1.44
High	1362.08	7.70	33	16.02	2.08
Very High	982.55	10.33	76	36.89	3.57
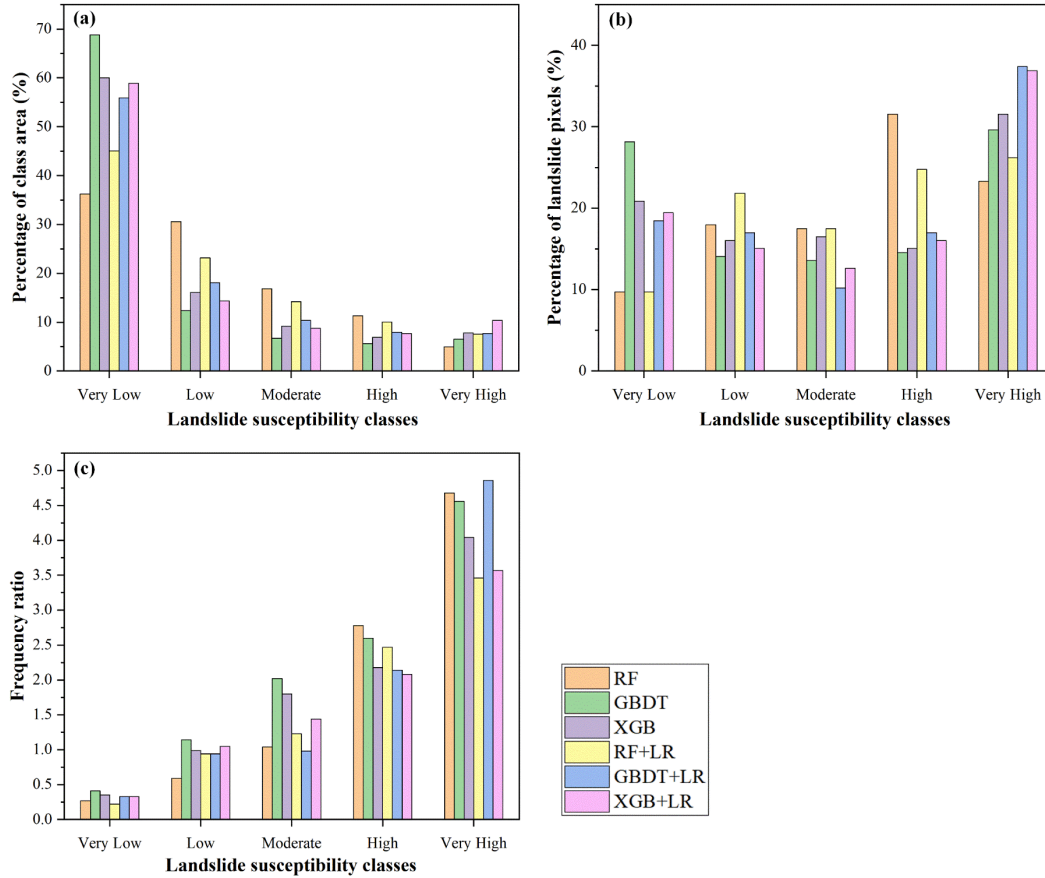
Fig 7. Frequency ratio (FR) analysis of landslide susceptibility maps: (a) percentage of class area (%), (b) percentage of landslide occurrences (%), and (c) FR.

We chose the GBDT+LR model with the best model performance and FR analysis result to verify its actual predictive ability. Several landslide instances, extracted from Google Earth (www.google.com, Mountain View, USA), coincide with areas predicted to have high and very high landslide susceptibility (Fig. 8), which shows that the results predicted by the GBDT+LR model are highly consistent with the actual situation.
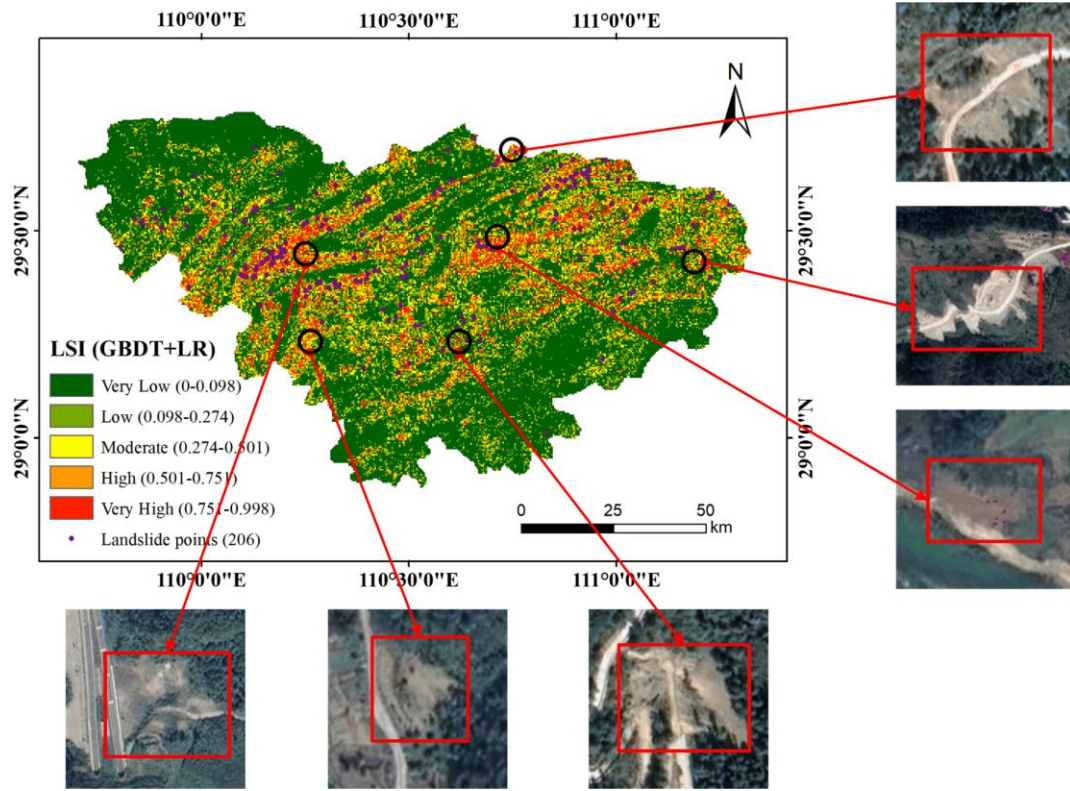
Figure 8. Landslide instances (extracted from Google Earth) in areas of high and very high landslide susceptibility predicted by the GBDT+LR.

5. Discussion

Landslides in Zhangjiajie City, Hunan Province, China, have received considerable attention. LSM is of great significance for visually analyzing landslide susceptibility. The main goal of this study was to stack several DT-based classifiers with a LR classifier to generate RF+LR, GBDT+LR, and XGB+LR models to obtain the optimal model for the study area, and to compare them with individual RF, GBDT, and XGB classifiers. Subsequently, they were applied in LSM in Zhangjiajie City, Hunan Province, China.

In LSM, it is important to evaluate the predictive capability of all LCFs. Factor choosing and sorting methods mainly include filter, wrapper, and embedded methods, and the IGR technique is a typical filter. In this study, we used the IGR technique to identify the LCFs' predictive capacity. The weight of each LCF was calculated using the entropy index. The AM values of 15 LCFs were tested to be greater than 0, indicating varying impacts of landslides in the study area. We demonstrated that profile curvature, roughness, LULC, altitude, distance to roads, TWI, and lithology are more important LCFs for LSM. In contrast, NDVI, slope, distance to rivers, plane curvature, aspect, soil textures, and rainfall were found to be less important in the study area. A systematic review of the literature shows that the importance of LCFs is specific to a region and cannot be extrapolated to other regions. For instance, Nhu et al. (2020b) identified rainfall as most important gully erosion factor in the Salavat

Abad saddle, Kurdistan Province, Iran. However, Pham et al. (2020b) discovered that slope is the most influential factor in the Muong Lay district in Vietnam. The study of Zhao et al. (2021) showed that the TWI is the most important LCF in Longnan City, Gansu Province, China.

After choosing suitable LCFs, we used six machine learning models to predict the landslide susceptibility maps. According to the evaluation results of the model performances, XGB was better than GBDT and RF, and the stacking ensemble learning techniques improved the goodness-of-fit and performances of these models. The model performance of GBDT+LR was better than RF+LR and XGB+LR. In particular, for RF and GBDT, the results after stacking fusion with LR were better than for RF and GBDT alone, respectively. However, XGB alone was better than XGB+LR. This is inconsistent with our expectations for two possible reasons: (1) a simple stacking ensemble process of XGB model will not necessarily improve its performance; and (2) when there are not enough training samples, the effect of XGB + LR tends to deteriorate. In addition, it is not always the case that the modeling performance of a fusion model is better than that of a single model. Zhou et al. (2021a) used XGB, RF, GBDT, LR, XGB + LR, RF + LR, and GBDT + LR models to study lymph node metastasis (LNM) in patients with poorly differentiated-type intramucosal gastric cancer, and suggested that a single machine learning algorithm can predict LNM, and that a fusion algorithm cannot improve the performance of machine learning in predicting LNM.

Five landslide susceptibility levels were obtained in the ultimate phase by dividing the LSI (0 to 1) using the natural break method. The selection of partitioning methods determines the correctness of LSM. Natural breaks, standard deviations, equal intervals, and quantiles have been used in LSM. Among them, the natural break method is considered the most popular method, and different classes can be generated based on the inherent characteristics of the dataset without any subjective consideration (Chen and Zhang, 2021). As shown in Fig. 7c, among all LSMs obtained in this study, the largest FR value belongs to the very high susceptibility category, followed by the high, moderate, low and very low susceptibility categories, proving that the models have the ability to effectively discriminate landslide occurring areas with different levels of susceptibility. The results also show that the prediction abilities of the percentage and FR of landslide occurrences are more reasonable with the stacking improvement in LSM.

The GBDT+LR model is considered to be the most effective prediction model, and it classified approximately 7.93% and 7.69% of the land into high and very high susceptibility categories, respectively (Fig. 7a). The landslide-prone areas of the Zhangjiajie City are distributed in the central and western mountainous areas, and the distribution pattern is consistent with the trend of mountains. The results suggest that at least 15.62% of

the area requires early warning-related preventive measures to enable local authorities to take timely and appropriate action to avoid or reduce the impact of landslides.

6. Conclusions

We introduced six DT-based ensemble frameworks (RF, GBDT, XGB, RF+LR, GBDT+LR, and XGB+LR) for LSM models with good performances in Zhangjiajie City, Hunan Province, China. The multicollinearity analysis was effectively able to minimize the LSM model bias, and the IGR analysis was able to independently assess the LCFs' correlation and eliminate redundant LCFs. Machine learning provides efficient approaches for data-driven landslide susceptibility mapping. Stacking ensemble of machine learning methods can effectively improve the model's goodness-of-fit and prediction performance. The DT-based models were used to build the stacking structures, and the stronger expressive ability of multiple DTs was better able to discover the effective features and feature combinations. The following conclusions can be drawn from the results:

(1) According to the AM values obtained using IGR technology, the profile curvature, roughness, LULC, altitude, distance to roads, TWI, and lithology are considered to be the most important influencing LCFs on landslides in the study area.

(2) All DT-based models showed good performance, among which the AUC value of the stacking ensemble GBDT+LR model reached 0.8168, showing the best prediction ability compared with the other models. The results of RF and GBDT stacking with LR were better than RF and GBDT alone, respectively; however, XGB+LR stacking cannot significantly improve the prediction accuracy.

(3) The results of the FR analysis indicate that low and very low landslide susceptibility categories account for the largest proportion in the study area, and a large proportion of historical landslide points are distributed in high and very high susceptibility areas. The landslide occurrences and frequency of landslides in the high and very high susceptibility categories generated by the GBDT+LR model are higher than those of other models. The LSM result of the GBDT+LR model has the best reliability, and can thus help decision-makers in large-scale land-use planning and geological disaster prevention.

(4) The stacking ensemble strategy shows many advantages. First, it can effectively combat overfitting by adding a regular term, and it does not require much parameter tuning or feature selection. Second, it uses multi-fold cross-validation to make the model more robust. In addition, it can re-integrate the methods to achieve better results. However, the stacking ensemble strategy has low stability and error accumulation shortcomings in practice, and it was not effective for the XGB method in this study. In future, we will attempt to further solve these problems, focusing on the development of ensemble machine learning technology and deep learning technology in LSM.

Acknowledgments: The authors thank the MapGIS Laboratory Co-Constructed by National Engineering Research Center for Geographic Information System of China and Central South University for providing MapGIS® software (Wuhan Zondy Cyber-Tech Co. Ltd., Wuhan, China). We also thank Mr. Dongliang Huang (Senior Engineer at the Hunan Provincial Planning Institute of Land and Resources) and Dr. Lifang Wang (Engineer at the Hunan Vocational College of Engineering) for providing and processing the dataset.

Conflicts of Interest: The authors declare no conflicts of interest.

Figure captions

Fig. 1 Location map of the study area: (a) location of the study area in Hunan Province, and (b) elevation of the study area along with location of historical landslide points.

Fig. 2 LCFs for landslide susceptibility mapping (LSM): (a) altitude, (b) slope, (c) aspect, (d) plane curvature, (e) profile curvature, (f) relief, (g) roughness, (h) rainfall, (i) topographic wetness index (TWI), (j) normalized difference vegetative index (NDVI), (k) distance to roads, (l) distance to rivers, (m) land use/land cover (LULC), (n) soil texture, and (o) lithology.

Fig. 3 Flowchart of LSM using the stacking ensemble machine learning models.

Fig. 4 Stacking ensemble structures for random forest (RF), gradient boosting decision tree (GBDT), and Extreme gradient boosting (XGB) with logistic regression (LR).

Fig. 5 Receiver operating characteristic (ROC) curves of the LSM models.

Fig. 6 Landslide susceptibility maps using: (a) RF, (b) GBDT, (c) XGB, (d) RF+LR, (e) GBDT+LR, and (f) XGB+LR models.

Fig. 7 Frequency ratio (FR) analysis of landslide susceptibility maps: (a) percentage of class area (%), (b) percentage of landslide occurrences (%), and (c) FR.

Fig. 8 Landslide instances (extracted from Google Earth) in areas of high and very high landslide susceptibility predicted by the GBDT+LR.

Table captions

Table 1 The landslide conditioning factors (LCFs) used in this study.

Table 2 Lithological units and their description of the study area.

Table 3 Multicollinearity of the LCFs.

Table 4 The most effective factors for landslide occurrence.

Table 5 Hyper-parameters of basic classifiers.

Table 6 Evaluation of LSM models using machine learning metrics.

Table 7 Evaluation of LSM models using error metrics.

Table 8 Statistics of landslide susceptibility classes with frequency ration (FR).

References

Abedini M, Tulabi S (2018) Assessing LNRF, FR, and AHP models in landslide susceptibility mapping index: a comparative study of Nojian watershed in Lorestan province, Iran. ENVIRONMENTAL EARTH SCIENCES 77(11):1-13

Aghdam I N, Pradhan B, Panahi M (2017) Landslide susceptibility assessment using a novel hybrid model of statistical bivariate methods (FR and WOE) and adaptive neuro-fuzzy inference system (ANFIS) at southern Zagros Mountains in Iran. ENVIRONMENTAL EARTH SCIENCES 76(6):237

Althuwaynee O, Pradhan B, Park H-J, et al. (2014) A novel ensemble decision tree-based CHi-squared Automatic Interaction Detection (CHAID) and multivariate logistic regression models in landslide susceptibility mapping. Landslides 11(6):1063-1078

Arabameri A, Pradhan B, Rezaei K, et al. (2019) GIS-based landslide susceptibility mapping using numerical risk factor bivariate model and its ensemble with linear multivariate regression and boosted regression tree algorithms. Journal of Mountain Science 16(3):595-618

Arulbalaji P, Padmalal D, Sreelash K (2019) GIS and AHP techniques based delineation of groundwater potential zones: a case study from southern Western Ghats, India. Scientific Reports 9(1):1-17

Band S S, Janizadeh S, Chandra Pal S, et al. (2020) Novel Ensemble Approach of Deep Learning Neural Network (DLNN) Model and Particle Swarm Optimization (PSO) Algorithm for Prediction of Gully Erosion Susceptibility. Sensors 20(19):5609

Botzen W J W, Aerts J C J H, Van Den Bergh J C J M (2013) Individual preferences for reducing flood risk to near zero through elevation. Mitigation and Adaptation Strategies for Global Change 18(2):229-244

Breiman L (1996) Bagging Predictors. Machine Learning 24(2):123-140

Breiman L (2001) Random forests. Machine Learning 45(1):5-32

Chen T, Guestrin C (2016) Xgboost: A scalable tree boosting system. In: Proceedings of the 22nd acm sigkdd international conference on knowledge discovery and data mining. pp 785-794

Chen T, Zhu L, Niu R-Q, et al. (2020a) Mapping landslide susceptibility at the Three Gorges Reservoir, China, using gradient boosting decision tree, random forest and information value models. Journal of Mountain Science 17(3)

Chen W, Chen Y, Tsangaratos P, et al. (2020b) Combining Evolutionary Algorithms and Machine Learning Models in Landslide Susceptibility Assessments. Remote Sensing Vol.12(No.23):3854

Chen W, Zhang S (2021) GIS-based comparative study of Bayes network, Hoeffding tree and logistic model tree for landslide susceptibility modeling. Catena 203:105344

Cruden D M, Varnes D J (1996) Landslide types and processes. Special Report - National Research Council, Transportation Research Board 247:36-75

Demir G (2019) GIS-based landslide susceptibility mapping for a part of the North Anatolian Fault Zone between

Reşadiye and Koyulhisar (Turkey). Catena 183:104211

Dou J, Yunus A P, Bui D T, et al. (2020) Improved landslide assessment using support vector machine with bagging, boosting, and stacking ensemble machine learning framework in a mountainous watershed, Japan. Landslides 17(3):641-658

Farrar D E, Glauber R R (1967) Multicollinearity in regression analysis: the problem revisited. The Review of Economic and Statistics:92-107

Freund Y (1990) Boosting a Weak Learning Algorithm by Majority. Information and Computation 121(2):256-285

Gigović L, Drobnjak S, Pamučar D (2019) The application of the hybrid GIS spatial multi-criteria decision analysis best–worst methodology for landslide susceptibility mapping. ISPRS International Journal of Geo-Information 8(2):79

Green I R A, Stephenson D (1986) Criteria for comparison of single event models. Hydrological Sciences Journal 31(3):395-411

Guzzetti F, Galli M, Reichenbach P, et al. (2006) Landslide hazard assessment in the Collazzone area, Umbria, Central Italy. Nat. Hazards Earth Syst. Sci. 6(1):115-131

Guzzetti F, Reichenbach P, Cardinali M, et al. (2005) Probabilistic landslide hazard assessment at the basin scale. GEOMORPHOLOGY 72(1-4):272-299

He X, Pan J, Jin O, et al. (2014) Practical lessons from predicting clicks on ads at facebook. In: Proceedings of the Eighth International Workshop on Data Mining for Online Advertising. pp 1-9

Hong H, Naghibi S A, Pourghasemi H R, et al. (2016) GIS-based landslide spatial modeling in Ganzhou City, China. Arabian Journal of Geosciences 9(2):112

Huang F M, Chen J W, Du Z, et al. (2020) Landslide Susceptibility Prediction Considering Regional Soil Erosion Based on Machine-Learning Models. ISPRS International Journal of Geo-Information 9(6):377

Hunan Bureau of Geology and Mineral Resources (1988) Hunan Regional Geology. Geological Publishing House, Beijing

Hungr O, Leroueil S, Picarelli L (2014) The Varnes classification of landslide types, an update. Landslides 11(2):167-194

Jerome H F (2001) Greedy function approximation: A gradient boosting machine. The Annals of Statistics 29(5):1189-1232

Kadavi P R, Lee C W, Lee S (2019) Landslide-susceptibility mapping in Gangwon-do, South Korea, using logistic regression and decision tree models. ENVIRONMENTAL EARTH SCIENCES 78(4):116

Kalantar B, Pradhan B, Naghibi S A, et al. (2018) Assessment of the effects of training data selection on the landslide susceptibility mapping: a comparison between support vector machine (SVM), logistic regression (LR) and artificial neural networks (ANN). Geomatics, Natural Hazards & Risk 9(1):49-69

Lai J-S, Tsai F (2019) Improving GIS-based landslide susceptibility assessments with multi-temporal remote sensing and machine learning. Sensors 19(17):3717

Lin W, Yin K, Wang N, et al. (2021) Landslide hazard assessment of rainfall-induced landslide based on the CF-SINMAP model: a case study from Wuling Mountain in Hunan Province, China. Natural Hazards 106(1):679-700

Ma B, Gao R, Zhao B, et al. (2015) Disease prediction based on LR-RF method. Basic and Clinical Pharmacology and Toxicology 117:14

Merghadi A, Yunus A P, Dou J, et al. (2020) Machine learning methods for landslide susceptibility studies: A

comparative overview of algorithm performance. Earth-Science Reviews 207

Mondal S, Mandal S (2020) Data-driven evidential belief function (EBF) model in exploring landslide susceptibility zones for the Darjeeling Himalaya, India. Geocarto International 35(8):818-856

Nahayo L, Mupenzi C, Habiyaremye G, et al. (2019) Landslides Hazard Mapping in Rwanda Using Bivariate Statistical Index Method. Environmental Engineering Science 36(8):892-902

Nefeslioglu H A, Duman T Y, Durmaz S (2008) Landslide susceptibility mapping for a part of tectonic Kelkit Valley (Eastern Black Sea region of Turkey). GEOMORPHOLOGY 94(3/4):401-418

Nguyen V-T, Tran T H, Ha N A, et al. (2019) GIS based novel hybrid computational intelligence models for mapping landslide susceptibility: a case study at da lat city, Vietnam. Sustainability 11(24):7118

Nhu V-H, Janizadeh S, Avand M, et al. (2020a) Gis-based gully erosion susceptibility mapping: A comparison of computational ensemble data mining models. Applied Sciences 10(6):2039

Nhu V-H, Zandi D, Shahabi H, et al. (2020b) Comparison of support vector machine, Bayesian logistic regression, and alternating decision tree algorithms for shallow landslide susceptibility mapping along a mountainous road in the west of Iran. Applied Sciences 10(15):5047

Petley D (2012) Global patterns of loss of life from landslides. Geology 40(10):927-930

Pham B T, Bui D T, Indra P, et al. (2015) Landslide Susceptibility Assessment at a Part of Uttarakhand Himalaya, India using GIS – based Statistical Approach of Frequency Ratio Method. International Journal of Engineering & Technical Research V4(11):338-344

Pham B T, Phong T V, Nguyen-Thoi T, et al. (2020a) GIS-based ensemble soft computing models for landslide susceptibility mapping. Advances in Space Research 66(6)

Pham B T, Tien Bui D, Prakash I, et al. (2017) Hybrid integration of Multilayer Perceptron Neural Networks and machine learning ensembles for landslide susceptibility assessment at Himalayan area (India) using GIS. Catena 149:52-63

Pham B T, Van Phong T, Nguyen-Thoi T, et al. (2020b) GIS-based ensemble soft computing models for landslide susceptibility mapping. Advances in Space Research 66(6):1303-1320

Sadighi M, Motamedvaziri B, Ahmadi H, et al. (2020) Assessing landslide susceptibility using machine learning models: a comparison between ANN, ANFIS, and ANFIS-ICA. Environmental Earth Sciences 79(24):536

Sahin E K (2020) Assessing the predictive capability of ensemble tree methods for landslide susceptibility mapping using XGBoost, gradient boosting machine, and random forest. SN Applied Sciences 2(7):1-17

Sur U, Singh P, Meena S R (2020) Landslide susceptibility assessment in a lesser Himalayan road corridor (India) applying fuzzy AHP technique and earth-observation data. Geomatics, Natural Hazards and Risk 11(1):2176-2209

Thai Pham B, Tien Bui D, Prakash I (2018) Landslide susceptibility modelling using different advanced decision trees methods. Civil Engineering and Environmental Systems 35(1-4):139-157

Tien Bui D, Shahabi H, Omidvar E, et al. (2019) Shallow landslide prediction using a novel hybrid functional machine learning algorithm. Remote Sensing 11(8):931

Wang Y, Feng L, Li S, et al. (2020) A hybrid model considering spatial heterogeneity for landslide susceptibility mapping in Zhejiang Province, China. Catena 188:104425

Webb G I (2000) Multiboosting: A technique for combining boosting and wagging. Machine Learning 40(2):159-196

Wolpert D H (1992) Stacked generalization. Neural Networks 5(2):241-259

Yang G, Zhang X, Tian M, et al. (2011) Alluvial terrace systems in Zhangjiajie of northwest Hunan, China: Implications for climatic change, tectonic uplift and geomorphic evolution. Quaternary International 233(1):27-39

Zhang B, Li M, Li W, et al. (2021) Machine learning strategies for lithostratigraphic classification based on geochemical sampling data: A case study in area of Chahanwusu River, Qinghai Province, China. Journal of Central South University 28(5):1422-1447

Zhao B, Ge Y, Chen H (2021) Landslide susceptibility assessment for a transmission line in Gansu Province, China by using a hybrid approach of fractal theory, information value, and random forest models. ENVIRONMENTAL EARTH SCIENCES 80(12):441

Zhou C-M, Wang Y, Ye H-T, et al. (2021a) Machine learning predicts lymph node metastasis of poorly differentiated-type intramucosal gastric cancer. Scientific Reports 10(1):1-7

Zhou X, Wen H, Zhang Y, et al. (2021b) Landslide susceptibility mapping using hybrid random forest with GeoDetector and RFE for factor optimization. Geoscience Frontiers 12(5):101211